Available online at www.sciencedirect.com

ScienceDirect

Procedia Structural Integrity 35 (2022) 25–33

Structural Integrity Procedia

www.elsevier.com/locate/procedia

2nd International Workshop on Plasticity, Damage and Fracture of Engineering Materials

Ductile failure prediction during the flow forming process

Hande Vural[a], Can Erdoğan[a], Tevfik Ozan Fenercioğlu[b], Tuncay Yalçinkaya[a,*]

[a] *Department of Aerospace Engineering, Middle East Technical University, 06800 Ankara , Turkey*
[b] *Repkon Machine and Tool Industry and Trade Inc., 34980 Sile, Istanbul, Turkey*

Abstract

Flow forming is an incremental metal-forming technique used for manufacturing thin-walled seamless tubes where a hollow metal material flows axially along the mandrel by a rotating mandrel and multiple cylinders. Flow formed materials are frequently used in the aviation and defence industry and it is crucial to examine the influence of the process on the material in terms of ductile fracture. However, the process requires in-depth failure analysis considering different process parameters and materials. The current study is concerned with investigating the ductile fracture behavior during flow forming process which includes complex stress states in terms of stress triaxiality and Lode parameter. Ductile fracture is simulated through the modified Mohr-Coulomb model. A user material subroutine (VUMAT) has been developed to implement the plasticity behavior and the damage accumulation rule. The model is validated through finite element (FE) simulations performed in Abaqus/Explicit and using the experimental data in Granum et al. (2021). The validated framework is applied to a finite element model of flow forming process with single and three rollers. The incremental forming with three rollers significantly reduces the damage accumulation. The initial results show a highly damaged region outer and inner surfaces of the workpiece after 40% thickness reduction ratio, and the forming limit is predicted as about 40-45%. The modeling framework is planned to be applied using various process parameter for different materials.

Keywords: Flow forming process; Ductile fracture; Modified Mohr-Coulomb model

1. Introduction

Flow forming is a process in which the thickness a tube shaped material is reduced using the pressure applied by one or more rollers moving in the axial and circumferential directions. The length of the tube increases with decreasing thickness. Especially for the automotive and aviation industries, many important parts are shaped by the flow forming process. Some examples of the flow parts are rocket motor cases, hydraulic cylinders, high pressure vessels and launcher tubes. As indicated Marini et al. (2016), the process started to be preferred in the production of thin and lightweight parts due to its advantages such as simple tooling, low forming loads and low cost of the forming machine. A large range of materials (e.g. steel, titanium, aluminum and nickel) can be formed by flow forming. In

* T. Yalçinkaya Tel.: +90-312-210-4258 ; fax: +90-312-210-4250.
E-mail address: yalcinka@metu.edu.tr

10.1016/j.prostr.2021.12.044

addition, according to Wong et al. (2003), the flow forming process can produce parts with high mechanical properties, smooth surface quality and high geometrical accuracy. Moreover the process influence the microstructure evolution substantially (see e.g. Karakaş et al. (2021)) leading to interesting properties depending on the cross-section reduction ratio.

During the flow forming process, highly localized deformations occur in the material with a complex stress state; thus, the failure prediction during the process is a difficult task. Ductile fracture and the material flow instability such as diametral growth, waviness, and bulges are the most common failure types as indicated in Singh et al. (2021). Angle of attack of the roller, roller diameter, friction factor, feed rate and roller speed are some of the parameters of this process which are shown to influence the damage accumulation and failure of the the work piece.

Although there has been remarkable progress on the prediction of failure in ductile materials over the years, it is still a challenging area. A common approach is to use coupled or uncoupled continuum damage criteria to predict ductile failure using finite element (FE) analysis. In the coupled approach, the damage parameter and the constitutive equations are coupled so that the damage evolution affects the stress state (see eg. Gurson (1977); Tvergaard and Needleman (1984); Lemaitre (1985); Yalçinkaya et al. (2019a)). In the uncoupled one, the damage parameter does not influence the constitutive equations. Such models are utilize a fracture locus (see eg. Johnson and Cook (1985); Bai and Wierzbicki (2008)), which is usually a function of failure strain, stress triaxiality, and Lode parameter. Temperature and strain rate effects are also included in these models which are not considered in current study.

In the literature, there are limited amount of works that study the failure prediction during flow forming processes. In Depriester and Massoni (2014), Ma et al. (2015) and Xu et al. (2018), several theoretically derived failure criterion are used compared to predict the forming limits and study the effects of process parameters. These models does not include any calibration parameter and only the damage value at failure can be adjusted. It in concluded that Cockcroft-Latham (Cockroft and Latham, 1968) criteria can be a good and efficient candidate to predict failure in the flow forming process. Moreover, Singh et al. (2021) used a coupled approach with the Khan-Huang-Liang (KHL) (Khan et al., 2004) yield criteria with a continuous damage model based on the Lemaitre model. In their work, triple and single roller arrangements and the effect of feed rate on failure are investigated with FE analysis.

In the current study, the uncoupled approach with the modified Mohr-Coulomb (MMC) damage criteria which is initially proposed in Bai and Wierzbicki (2010) is followed. A variation of MMC damage criteria presented in Granum et al. (2021) is implemented as a user material subroutine in commercial FE software Abaqus. The model depends on stress triaxiality and Lode parameters and 6 calibration parameters. The material and calibration parameters are adopted from Granum et al. (2021). Then, the failure model is used in a FE simulation of a flow forming process to predict critical locations and the forming limits. The aim of the current work is to initialize a framework that can be used to predict the flow forming limits of several materials, and also study the effects of process parameters on failure.

2. Methods

2.1. Material

For this study, T6 temper of Al6016 aluminum alloy material was examined. Although this material has high strength and surface quality, its ductility is limited. It is a frequently used material in the automotive industry. Considering these properties, the ductile damage and fracture behavior of the material during the flow forming process is investigated. The test data, hardening and calibration parameters used throughout the study were taken from Granum et al. (2021).

Material is elasto-plastic with isotropic hardening and metal plasticity is described by the J_2 plasticity framework. The yield function is defined as $\Phi = \sigma_{eq} - \sigma_y$ where

$$\sigma_y = \sigma_0 + \sum_{i=1}^{3} Q_i(1 - exp(-C_i\bar{\varepsilon}_p)) \tag{1}$$

is the flow stress which is described by an extended Voce rule. $\sigma_{eq} = \sqrt{3J_2}$ is the von Mises equivalent stress and $\bar{\varepsilon}_p$ is the equivalent plastic strain. σ_0 is the initial yield stress and Q_i and C_i are material specific parameters. The yield stress and hardening parameters of materials are shown in Table 1. The density, Young's modulus and Poisson's ratio of AA6016-T6 aluminum alloy are taken as 2.7 g/cm^3, 70 GPa and 0.3, respectively.

Table 1: Material parameters of the extended Voce hardening rule.

E(GPa)	ν	σ_0(MPa)	Q_1(MPa)	C_1	Q_2(MPa)	C_2	Q_3(MPa)	C_3
70	0.3	254.1	6.45	438.98	109.39	11.13	2.58	9.05

The stress state may be described by two dimensionless parameters which are the stress triaxiality, T, and Lode parameter, L, as

$$T = \frac{\sigma_h}{\sigma_{eq}}, \; L = \sqrt{3}\tan\left(\theta_L - \frac{\pi}{6}\right) \tag{2}$$

where the hydrostatic stress is $\sigma_h = I_1/3$,where I_1 is first stress invariant and Lode parameter is described in terms of Lode angle, θ_L, which can be found from

$$\cos(3\theta_L) = \frac{J_3}{2}\left(\frac{3}{J_2}\right)^{3/2} \tag{3}$$

where J_2 and J_3 is second and third deviatoric stress invariant,respectively.

2.2. MMC Damage Criteria

Because of the nature of the flow forming, the material is exposed to compression, shear and tension at different stages of the process. It is decided that a variation of MMC model would be a suitable choice due to its dependence on stress triaxiality and Lode parameter. The model is defined as

$$\varepsilon_f(L,T) = \left\{\frac{K}{\hat{C}_2}\left[\hat{C}_3 + \frac{\sqrt{3}}{2-\sqrt{3}}(\hat{C}_4{}^* - \hat{C}_3)(\sec(\frac{-L\pi}{6}) - 1)\right] \times \left[\sqrt{\frac{1+\hat{C}_1{}^2}{3}}\cos\left(\frac{-L\pi}{6}\right) + \hat{C}_1\left(T + \frac{1}{3}\sin\left(\frac{-L\pi}{6}\right)\right)\right]\right\}^{-\frac{1}{n}} \tag{4}$$

where

$$\hat{C}_4{}^* = \begin{cases} 1 & \text{for } -1 \le L \le 0 \\ \hat{C}_4 & \text{for } 0 < L \le 1 \end{cases} \tag{5}$$

The model has six calibration parameters $\hat{C}_1, \hat{C}_2, \hat{C}_3, \hat{C}_4$, K and n and the values are given in Table 2 for the AA6016-T6.

Table 2: Calibrated parameters of the modified Mohr-Coulomb fracture model.

K	$\hat{C}_1$	$\hat{C}_2$	$\hat{C}_3$	$\hat{C}_4$	n
0.9988	0.01135	0.5081	0.8847	1.0066	0.01000

Damage evolution rule is expressed with the following integral

$$D = \int_0^{\bar{\varepsilon}_p} \frac{d\bar{\varepsilon}_p}{\varepsilon_f(L,T)} \tag{6}$$

Initially, the damage value is zero and the material is assumed to fail at $D = 1$.

2.3. Finite Element Modelling

The presented damage model is implemented in a user material model (VUMAT) for explicit FE simulations. Initially, 3 different specimens used in Granum et al. (2021) are modelled to verify current implementation. These specimens are notched tension with 10 mm radius (NT10), plane strain tension (PST) and in plane shear (ISS) specimen. By using the symmetry planes only a one-fourth of NT10 and PST specimens were modelled to shorten the FE solution time. 8-node linear brick elements (C3D8R) with reduced integration is used. At the critical sections, the mesh density is increased up to 10 elements in the thickness direction. The explicit solver of Abaqus is used and the failure is modelled with element deletion.

Calibrated and verified damage model is employed for the FE simulation of a backward flow forming analyses. The FE model is prepared with two different arrangements which are three rollers and single roller as shown in Fig. 1. These models are composed of a mandrel, preform and three and single roller. Mandrel and rollers are modelled as rigid bodies while preform tube is a deformable body. The rollers are rotating with respect the center of the mandrel and move in the axial direction of the preform. Three rollers are placed around the preform in the circumferential direction, with an angle of 120 degrees between them. Rollers are also placed with a certain spacing in the axial direction. The percent thickness reduction is controlled by moving the rollers in or out on the circumferential axis. In this way, the desired total thickness reduction percentage was obtained by decreasing the thickness of the workpiece gradually. Between the rollers and the preform tangential and normal contact is used. The preform tube is meshed with hexahedral elements with reduced integration (C3D8R) and hourglass control. Further, global mesh size is 1 mm and there are approximately 190000 elements in total. To reduce the computation time mass scaling is used, and the model is solved with dynamic explicit solver of Abaqus.

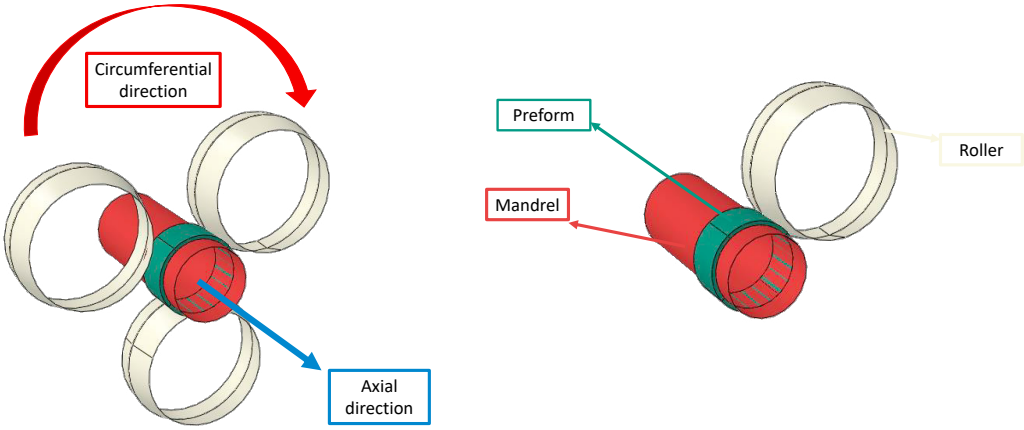

(a) 3 roller arrangement (b) Single roller arrangement

Fig. 1: Finite element models of flow forming process.

3. Results and Discussion

A notch tension, plane strain tension and in plane shear specimens are used to verify the calibrated parameters and accuracy of the MMC model with the implemented subroutine. Fig. 2 shows the force and displacement curves of the simulations. The black dots in the graphs show the experimental data from Granum et al. (2021). All figures are plotted up to failure. Damage accumulation just before the failure is shown visually for all 3 specimens. The results are found to be in agreement with both experimental data and the FE results presented in aforementioned study. It should be noted that the referenced study uses a high exponent Hershey-Hosford yield surface (see eg. Hosford (1972) and Hershey (1954)); however, in the current work, classical von Mises plasticity model is implemented.

The flow forming process is analysed in single roller and 3 roller configurations with different thickness reduction ratios. First of all, an appropriate thickness reduction value is decided based on the results in Karakaş et al. (2021). Thickness reduction ratios in the range of 10-50% are studied. In Fig. 3, the result of 15 seconds of flow forming simulation of the single-roller model with a thickening ratio of 40% is shown as full isometric, half isometric and side view. From this figure, it has been observed that the damage value of the inner surface of the flow formed material is higher than the outer surface ,and the maximum damage value is 0.853. The damage distribution for this model is homogeneous.

As discussed previously, different stress states such as tension, compression and shear affect the material during the flow forming process. In order to examine this situation, stress triaxiality (T), Lode (L) and damage parameter results are taken from 4 different elements shown in Fig. 4. Elements 1 and 3 are on the outer surface (in contact

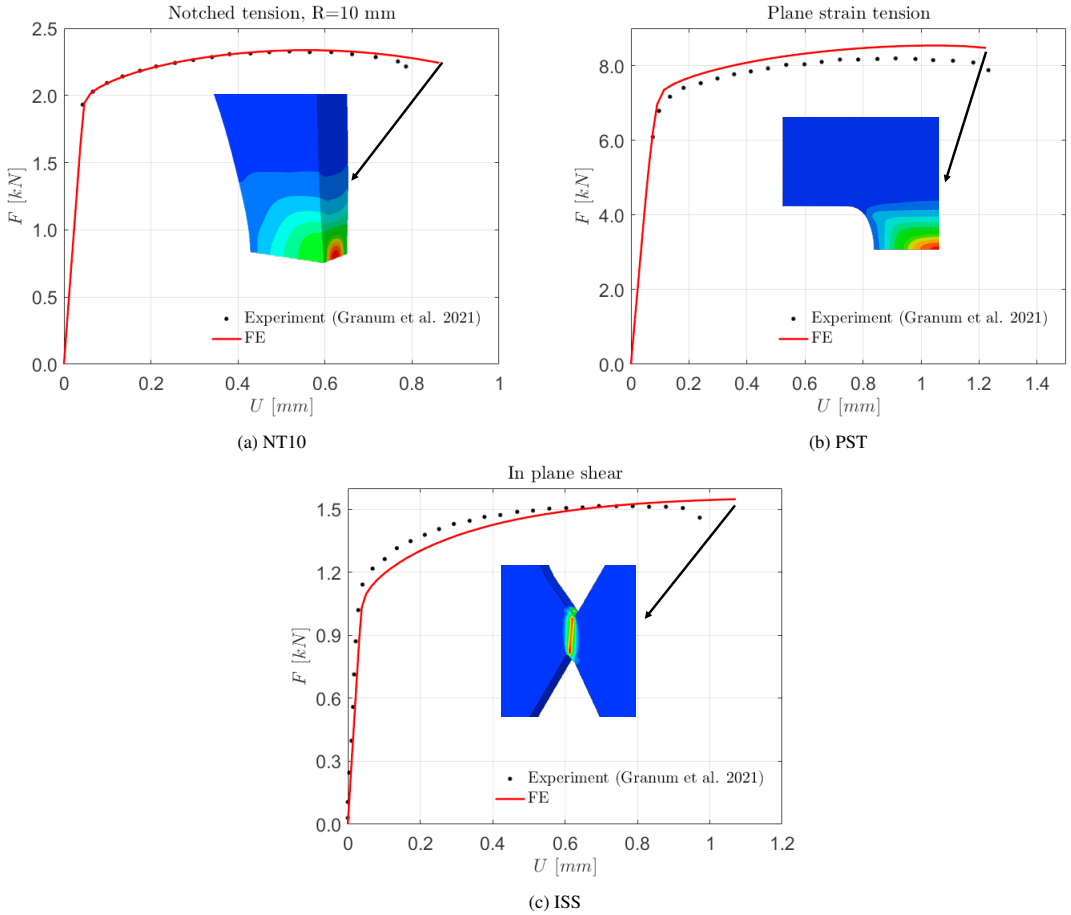

(a) NT10 (b) PST

(c) ISS

Fig. 2: Force-displacement curves of the failure simulations compared with the experimental data. All lines are plotted up to failure.

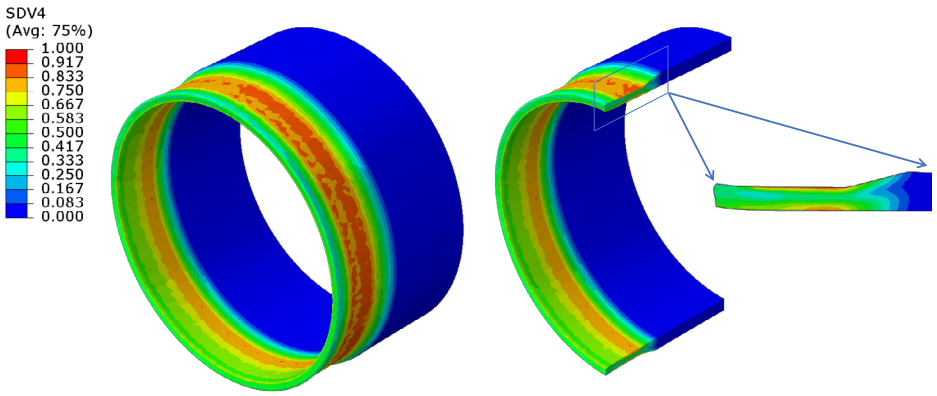

Fig. 3: Result of flow forming process for single roller and 40% thickness reduction ratio.

with rollers) while elements 2 and 4 are on the inner surface (in contact with mandrel). Element positions are selected based on critical locations. In Fig. 5, it can be observed that T and L values change significantly. During the process, T is found to be between -0.5 and 1, L values are changed in the range of -1 and 1. When the T and L distributions

of the elements on the inner and outer surfaces are examined, it is concluded that at the outer surface, elements are subject to more abrupt changes than the element at the inner surface. Nevertheless, a complex stress state is observed on both surfaces. When we look at the average T and L values in the graphs, both T and L values for elements 1 and 2 are close to zero. Unlike these two elements, T in element 3 and L in element 4 are higher 0. Element 3 is in a more critical location compared to others due to the higher average stress triaxiality.

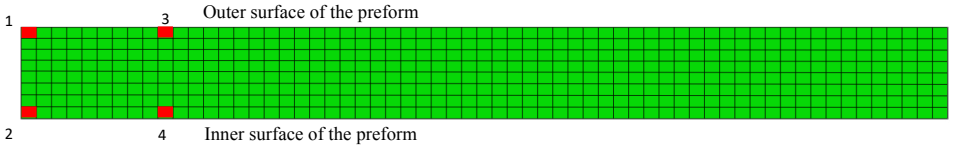

Fig. 4: Element output locations.

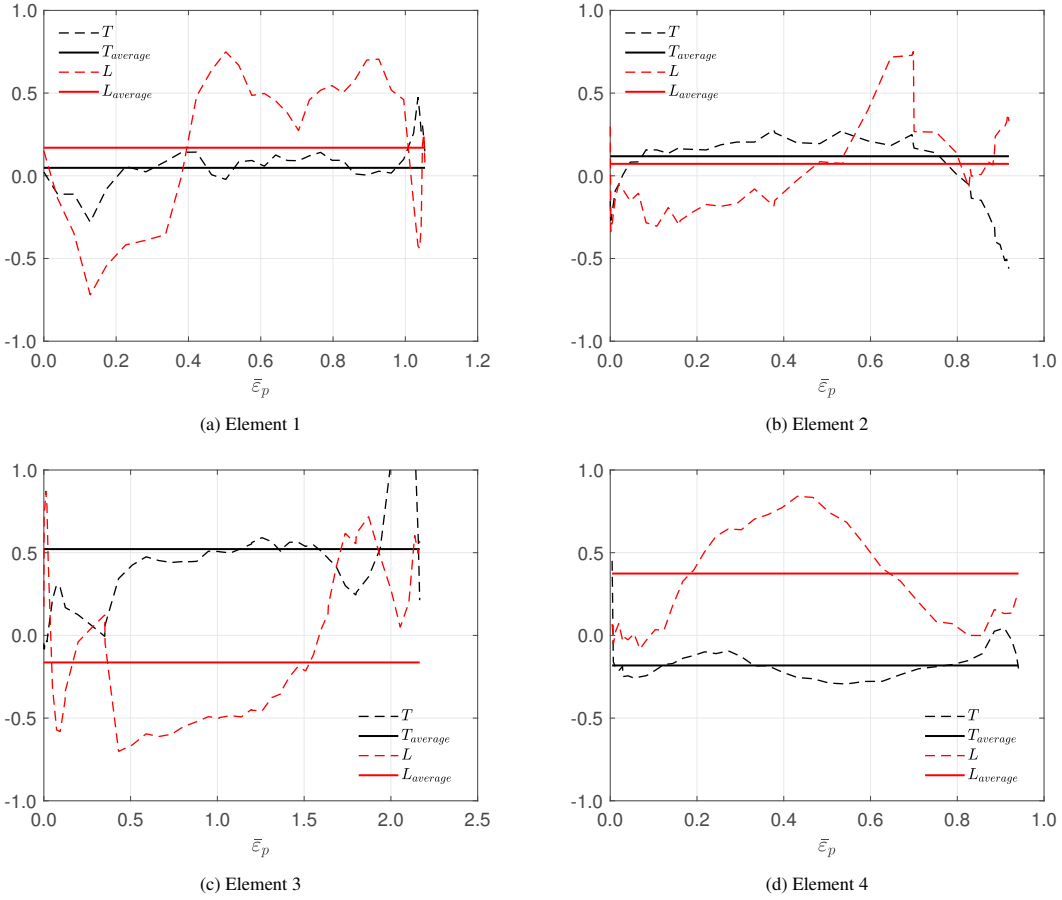

(a) Element 1

(b) Element 2

(c) Element 3

(d) Element 4

Fig. 5: Stress triaxiality and Lode parameter for single roller with 40% thickness reduction ratio.

In Fig 6, the change of damage values of 4 different elements selected for 40% and 50% thickness reduction ratio is shown. In Fig 6a, the damage value of all elements remained below one, and it is concluded that 40% is a thickness reduction ratio suitable for this material. When Fig 6b is examined, all selected elements except element 1 exceed the damage value of one. Reducing the thickness of the material used for the flow forming process by 50% resulted in failure.

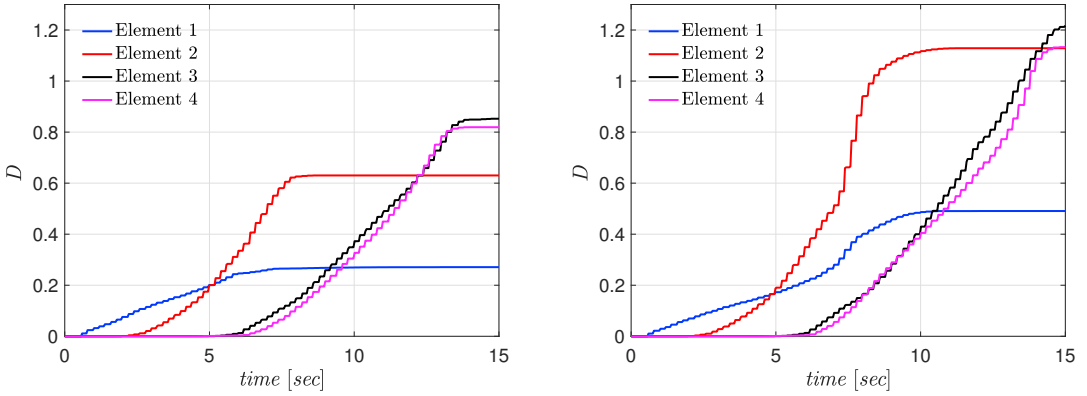

(a) Damage parameter for single roller with 40% thickness ratio

(b) Damage parameter for single roller with 50% thickness ratio

Fig. 6: Damage accumulation comparison throughout the forming process.

In Fig. 7, the damage change in single and three roller flow forming is compared for the same thickness reduction ratio. The purpose of making three rollers flow forming is to incrementally reduce the thickness of the workpiece, which is shown to reduce the damage accumulation in Singh et al. (2021). In Fig. 7, the flow forming process, which is done with single rollers, reaches higher damage values at both first and second element location. Although both models had the same thickness reduction ratio, analysis with the three rollers model resulted in 25% and 44% less damage accumulation for element 1 and 2, respectively.

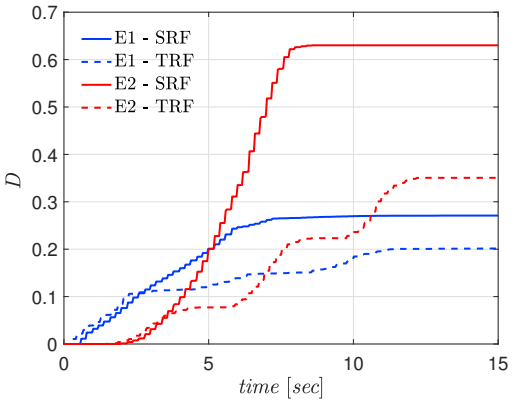

Fig. 7: Damage comparison in single roller (SRF) and 3 roller forming (TRF) configurations with 40% thickness reduction ratio in elements 1 and 2.

Five different flow forming analyses are carried out with 10 to 50% thickness reduction ratios. The damage distributions for these 5 different analyses are shown in 8. Damage varies from 10% to 50%, both in value and the distribution through the thickness. While the thickness reduction ratio is 10% and 20%, the damage is found to be higher on the inner surfaces, while the damage accumulation is high on both the inner and outer surfaces at 25% and higher thickness reduction ratios. From these analysis, a 40-45% thickness reduction is expected to be the limit for AL6016-T6 material with a single roller. Moreover, with 50% thickness reduction, curving of the left side of the workpiece becomes noticeable compared to lower thickness reduction values. It should be noted that these results are affected by other parameters such as friction coefficient, feed rate and rotational speed of rollers, which are not studied in the current work.

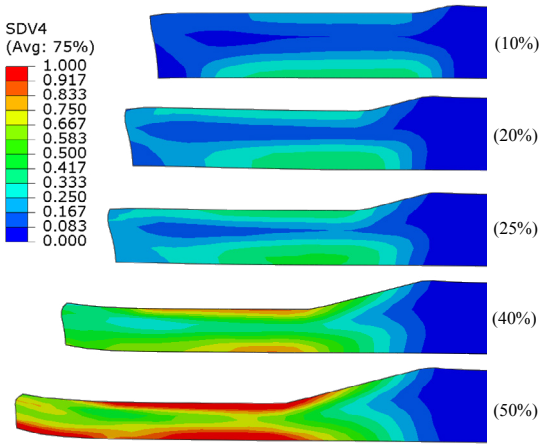

Fig. 8: Damage distribution of 10%, 20%, 25%, 40% and 50% thickness reduction with single roller flow forming.

4. Conclusion

This study presented an initial attempt on the failure estimation during a flow forming process using finite element analysis and the MMC failure criteria. The failure model is adopted from the literature and the implementation of the model is verified with experimental data. Then, the model is employed in the FE simulation of a backward flow forming process with single and three rollers. Based on the stress triaxiality and Lode parameter of 4 locations on the preform, critical locations for the damage accumulation is discussed. The elements on the outer surface which are in contact with rollers are found to be more critical. Moreover, it is shown that incrementally reducing the thickness with three rollers reduces the damage accumulation significantly. It is seen that 50% thickness reduction ratio results in failure for the aluminum alloy. However, it should be noted that there are several parameters such as friction, roller speed, feed rate in flow forming process which are expected to change failure behavior. Such parameters are planned to be studied in the near future with the through current framework. In addition to the macroscopic observations, flow forming process in known to change the microstructure of the preform and potentially create an anisotropic structure (see e.g. Wang et al. (2018); Zeng et al. (2020)). The influence of the such microstructure evolution is planned to be studied as well through crystal plasticity FE simulations (e.g. Yalçinkaya (2016); Yalçinkaya et al. (2019b, 2021)).

Acknowledgements

The authors gratefully acknowledge the support of Repkon Machine and Tool Industry and Trade Inc.

References

Bai, Y., Wierzbicki, T., 2008. A new model of metal plasticity and fracture with pressure and Lode dependence. International Journal of Plasticity 24, 1071–1096.

Bai, Y., Wierzbicki, T., 2010. Application of extended mohr-coulomb criterion to ductile fracture. International Journal of Fracture 161, 1–20.

Cockroft, M.G., Latham, D.J., 1968. Ductile and the workability of metals. Journal of the Institute of Metal 96, 33–39.

Depriester, D., Massoni, E., 2014. On the damage criteria and their critical values for flowforming of ELI grade Ti64, in: Metal Forming, pp. 1221–1227.

Granum, H., Morin, D., Børvik, T., Hopperstad, O.S., 2021. Calibration of the modified Mohr-Coulomb fracture model by use of localization analyses for three tempers of an AA6016 aluminium alloy. International Journal of Mechanical Sciences 192, 106122.

Gurson, A.L., 1977. Continuum theory of ductile rupture by void nucleation and growth. Journal of Engineering Materials and Technology 99, 2–15.

Hershey, A.V., 1954. The plasticity of an isotropic aggregate of anisotropic face-centered cubic crystals. Journal of Applied Mechanics 21, 241–249.

Hosford, W.F., 1972. A generalized isotropic yield criterion. Journal of Applied Mechanics 39, 607–609.

Johnson, G.R., Cook, W.H., 1985. Fracture characteristics of three metals subjected to various strains, strain rates, temperatures and pressures. Engineering Fracture Mechanics 21, 31–48.

Karakaş, A., Fenercioğlu, T.O., Yalçinkaya, T., 2021. The influence of flow forming on the precipitation characteristics of Al2024 alloys. Materials Letters 299, 130066.

Khan, A.S., Suh, Y.S., Kazmi, R., 2004. Quasi-static and dynamic loading responses and constitutive modeling of titanium alloys. International Journal of Plasticity 20, 2233–2248.

Lemaitre, J., 1985. Coupled elasto-plasticity and damage constitutive equations. Computer Methods in Applied Mechanics and Engineering 51, 31–49.

Ma, H., Xu, W., Jin, B.C., Shan, D., Nutt, S.R., 2015. Damage evaluation in tube spinnability test with ductile fracture criteria. International Journal of Mechanical Sciences 100, 99–111.

Marini, D., Cunningham, D., Xirouchakis, P., Corney, J.R., 2016. Flow forming: A review of research methodologies, prediction models and their applications. International Journal of Mechanical Engineering and Technology 7, 285–315.

Singh, A.K., Kumar, A., Narasimhan, K.L., Singh, R., 2021. Understanding the deformation and fracture mechanisms in backward flow-forming process of Ti-6Al-4V alloy via a shear modified continuous damage model. Journal of Materials Processing Technology 292, 117060.

Tvergaard, V., Needleman, A., 1984. Analysis of the cup-cone fracture in a round tensile bar. Acta Metallurgica 32, 157–169.

Wang, X.X., Zhan, M., Fu, M.W., Gao, P.F., Guo, J., Ma, F., 2018. Microstructure evolution of Ti-6Al-2Zr-1Mo-1V alloy and its mechanism in multi-pass flow forming. Journal of Materials Processing Technology 261, 86–97.

Wong, C.C., Dean, T.A., Lin, J., 2003. A review of spinning, shear forming and flow forming processes. International Journal of Machine Tools and Manufacture 43, 1419–1435.

Xu, W., Wu, H., Ma, H., Shan, D., 2018. Damage evolution and ductile fracture prediction during tube spinning of titanium alloy. International Journal of Mechanical Sciences 135, 226–239.

Yalçinkaya, T., 2016. Strain gradient crystal plasticity: thermodynamics and implementation, in: Handbook of Nonlocal Continuum Mechanics for Materials and Structures, pp. 1001–1033.

Yalçinkaya, T., Erdoğan, C., Tandoğan, I.T., Cocks, A., 2019a. Formulation and implementation of a new porous plasticity model. Procedia Structural Integrity 21, 46–51.

Yalçinkaya, T., Özdemir, I., Firat, A.O., 2019b. Inter-granular cracking through strain gradient crystal plasticity and cohesive zone modeling approaches. Theoretical and Applied Fracture Mechanics 103, 102306.

Yalçinkaya, T., Özdemir, I., Tandoğan, I.T., 2021. Misorientation and grain boundary orientation dependent grain boundary response in polycrystalline plasticity. Computational Mechanics 67, 937–954.

Zeng, X., Fan, X.G., Li, H.W., Zhan, M., Li, S.H., Wu, K.Q., Ren, T.W., 2020. Heterogeneous microstructure and mechanical property of thin-walled tubular part with cross inner ribs produced by flow forming. Materials Science and Engineering: A 790, 139702.